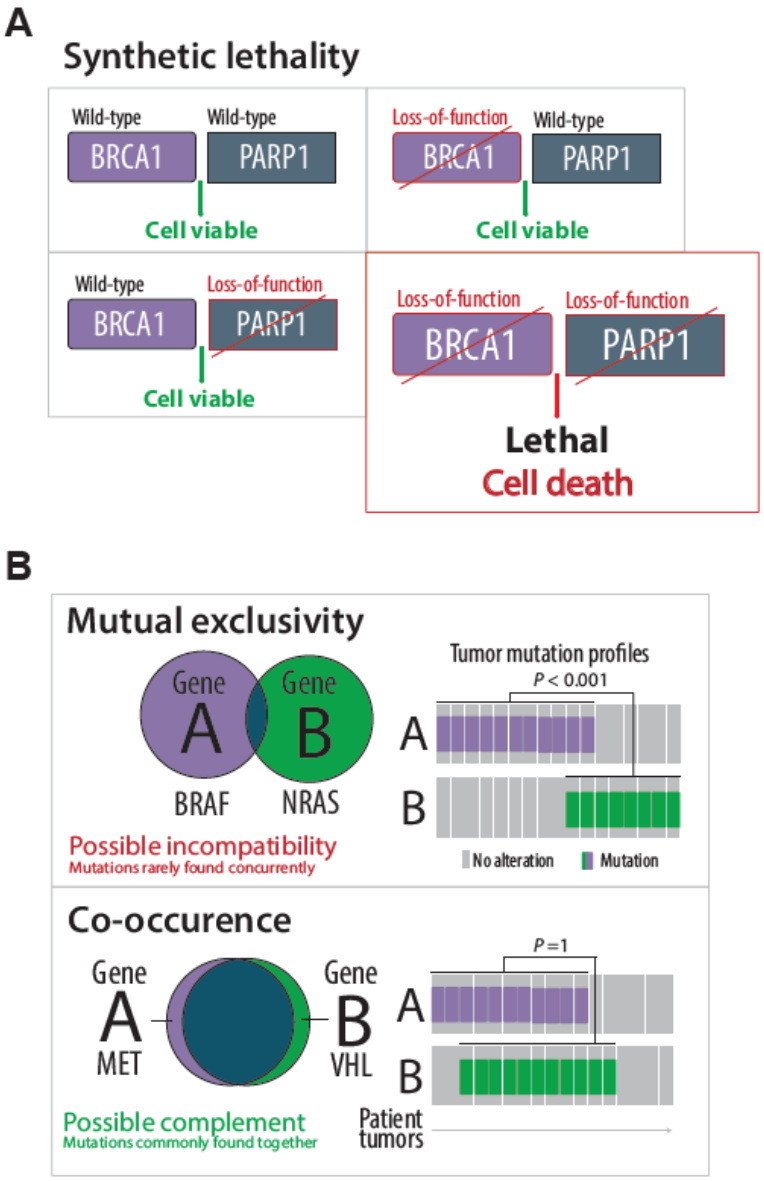

Supplementary Figure 1. Schematic illustrating genetic interaction concepts relevant to cancer genomics.
A) Illustration of synthetic lethality (SL). Loss-of-function in either *BRCA1* or *PARP1* alone does not impact cell viability, but concurrent loss-of-function in both genes results in cell death.
B) Mutual exclusivity and co-occurrence of gene mutations. The upper panel illustrates mutual exclusivity, where mutations in genes such as *BRAF* and *NRAS* rarely occur together due to functional incompatibility. The lower panel shows co-occurrence, where mutations in genes such as *MET* and *VHL* commonly occur simultaneously within tumors.

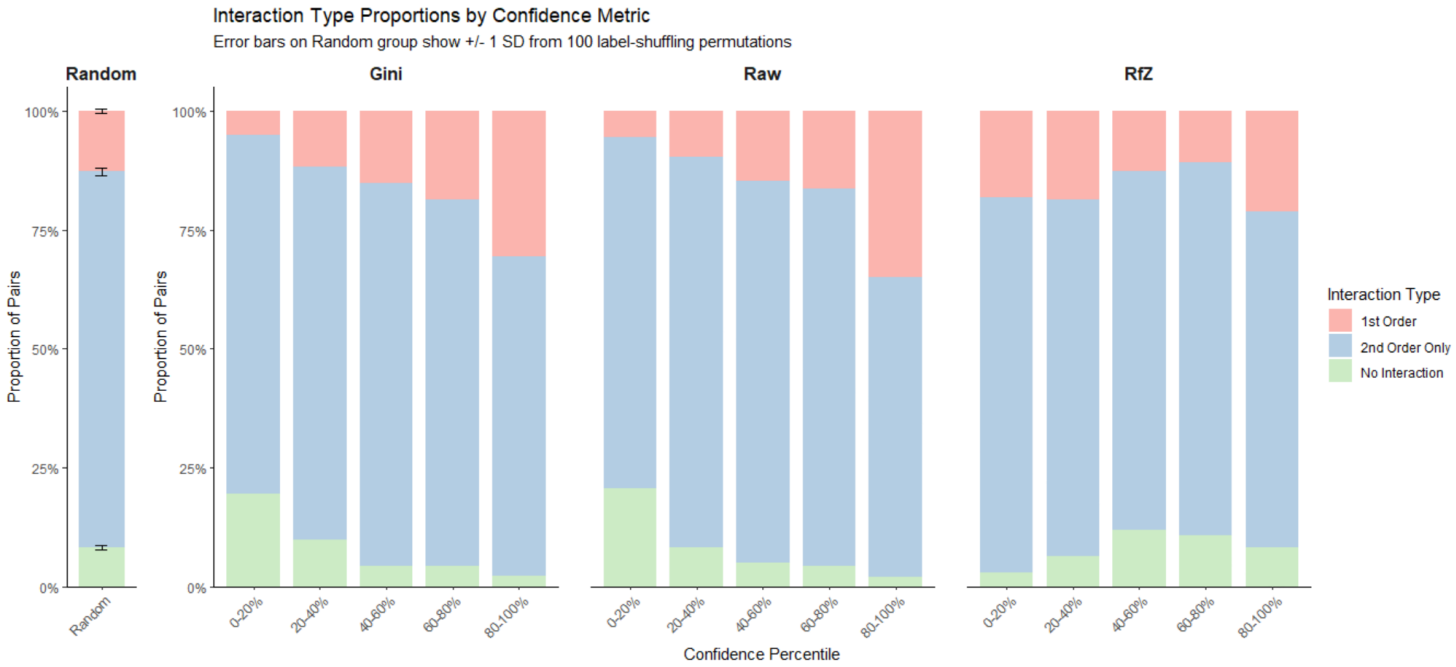

Supplementary Figure 2. Validation of feature selection through protein-protein interaction (PPI) enrichment. The bar plots show the proportion of predicted SL pairs that correspond to known PPIs from the STRING database. These interactions are categorized as direct (1st order), indirect through a shared partner (2nd order only), or having no known interaction. The leftmost 'Random' panel serves as a baseline, showing the proportions from 100 label-shuffling permutations (error bars represent ±1 standard deviation). The subsequent panels ('Gini', 'Raw', and 'RfZ') display the proportions for genetic interactions identified by the three Boruta importance metrics, binned by increasing confidence percentile. A strong positive correlation is observed between model confidence and the likelihood that the gene pairs have a known physical interaction, confirming that the feature selection method effectively prioritizes biologically meaningful signals over statistical noise.

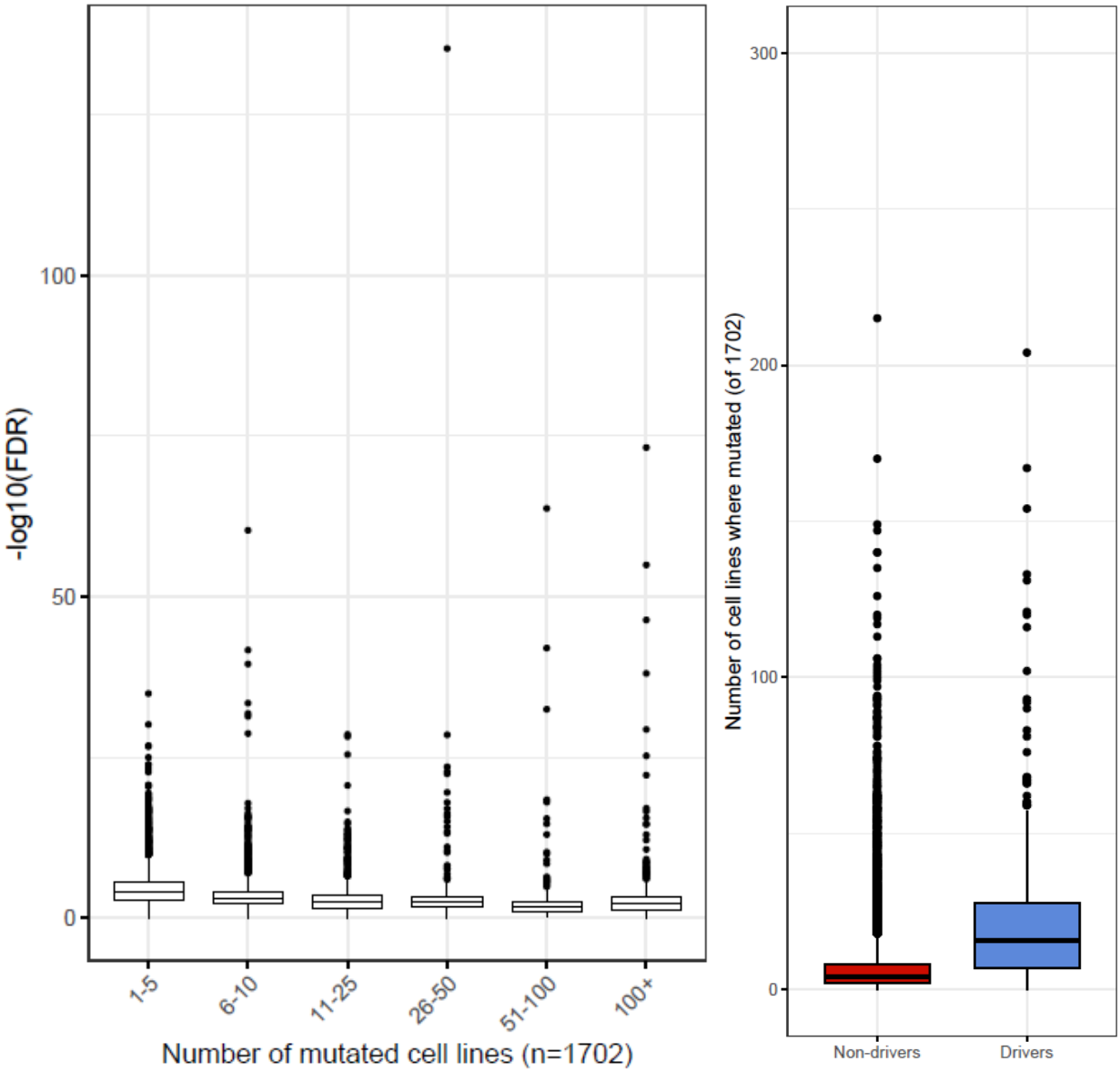

Supplementary Figure 3. Distribution of synthetic lethal (SL) interaction significance values stratified by mutation frequency across cell lines. **Left)** The relationship between the statistical significance of SL interactions (-log10(FDR)) and the number of mutated cell lines. **Right)** The mutation frequency in driver versus non-driver genes. SL interaction significance remains robust and stable regardless of mutation frequency, indicating that identified interactions are not artifacts of mutation prevalence differences.

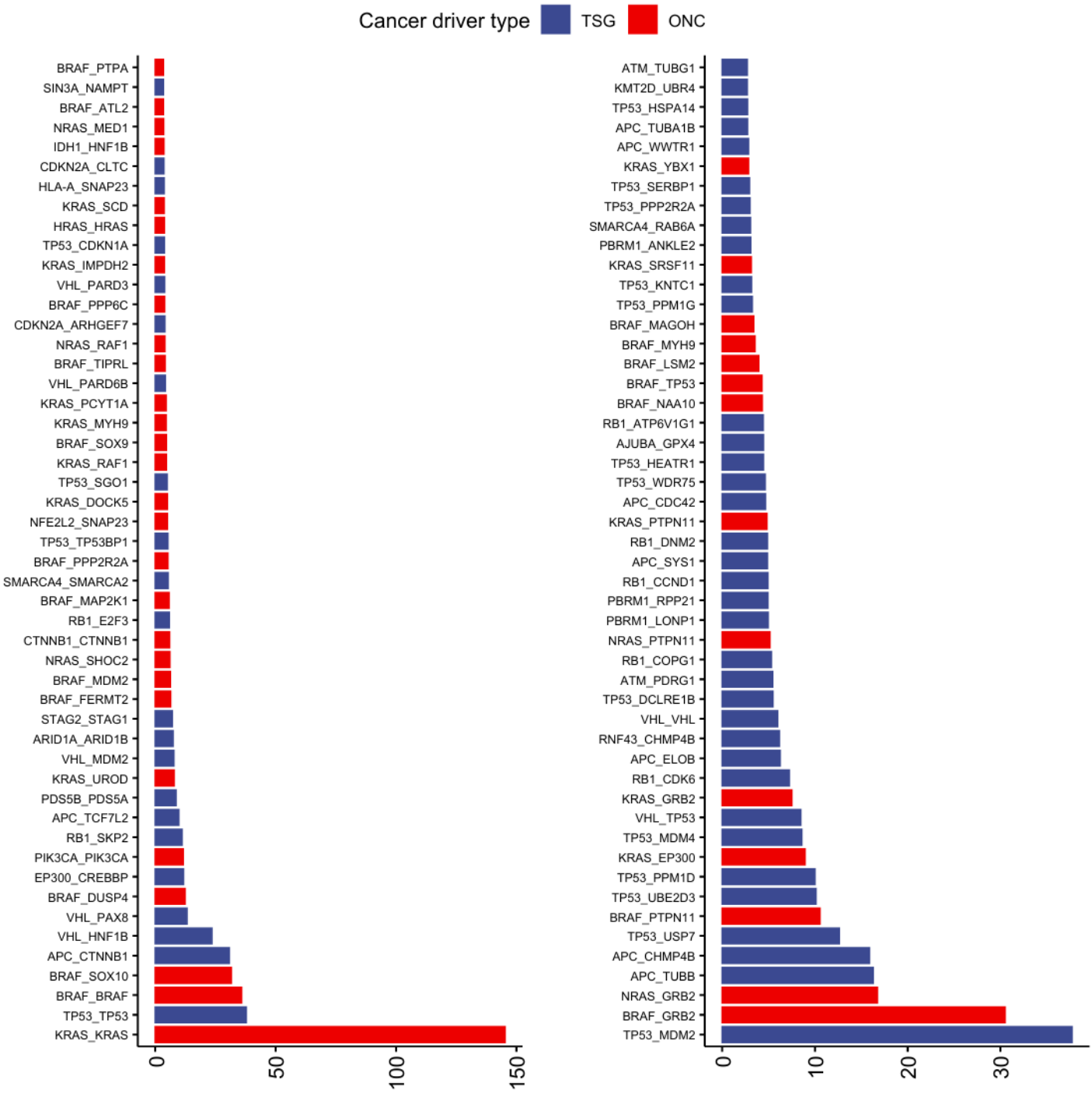

Supplementary Figure 4. Overview of pan-cancer synthetic lethal (SL, **left**) and resistance (**right**) genetic interactions identified in the analysis. Interactions are ranked according to their Gini importance value. Each bar represents an interaction between two cancer driver genes, classified as tumor suppressor genes (TSG; blue) or oncogenes (ONC; red). The first gene in each label is the source gene mutated in the cell line, while the second gene is knocked out via CRISPR. The extensive identification of well-known and experimentally validated genetic dependencies demonstrates the biological relevance and robustness of the analytical approach.

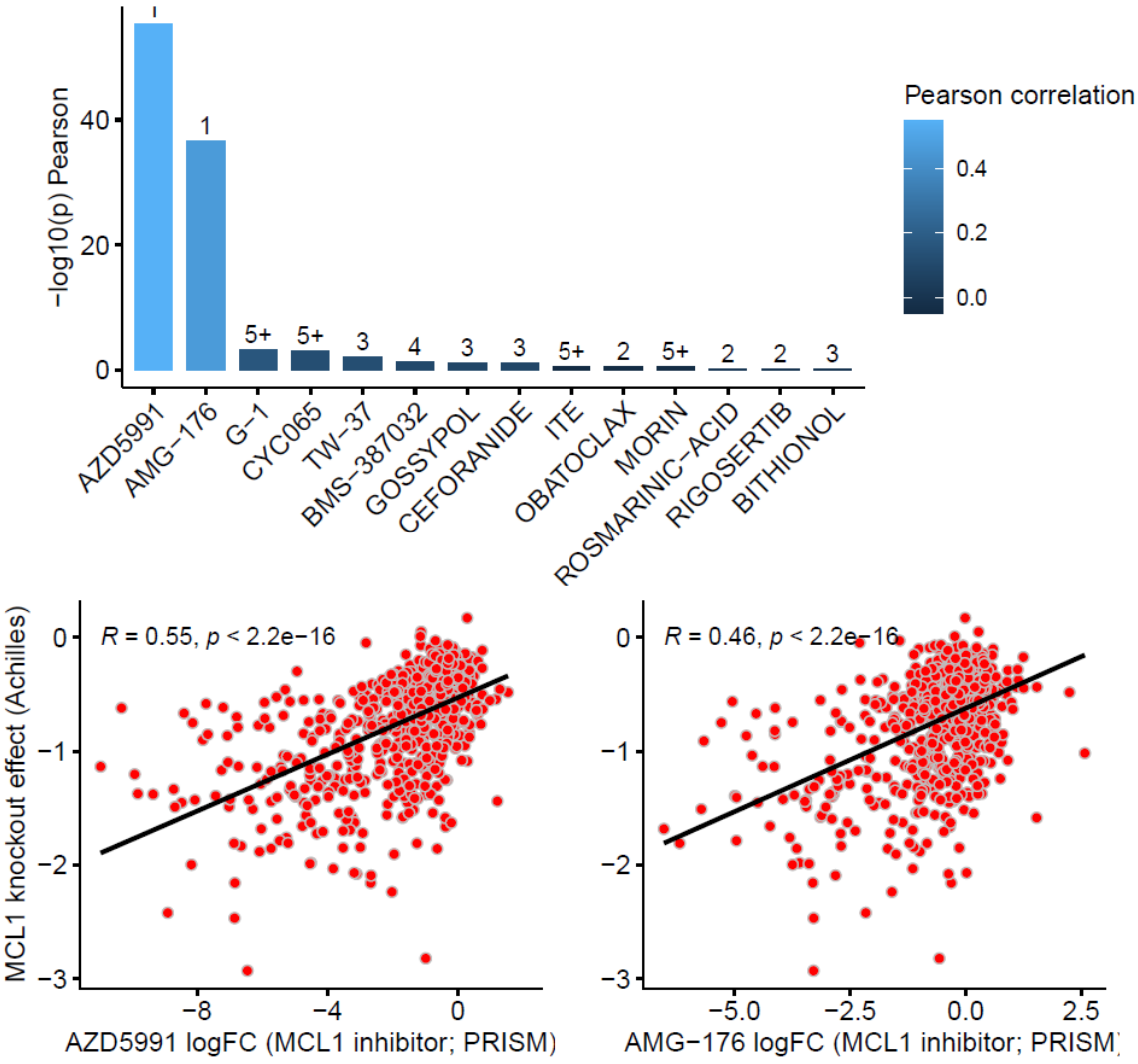

Supplementary Figure 5. Correlation of drug sensitivity with genetic dependency profiles for MCL1 inhibitors. **Top**) Drugs ranked by significance (-log10(p-value)) of correlation between their drug sensitivity profiles (PRISM) and MCL1 CRISPR knockout effect (DepMap). Bar color intensity represents Pearson correlation strength, and numbers above bars indicate the number of putative targets for each drug. **Bottom)** Scatter plots showing correlations between sensitivity to MCL1 inhibitors (AZD5991 (**left**) and AMG-176 (**right**); PRISM log fold-change) and the corresponding genetic dependency score from MCL1 knockout. Strong, statistically significant correlations support the biological specificity of these drug-gene interactions (P < 2.2e-16).

.

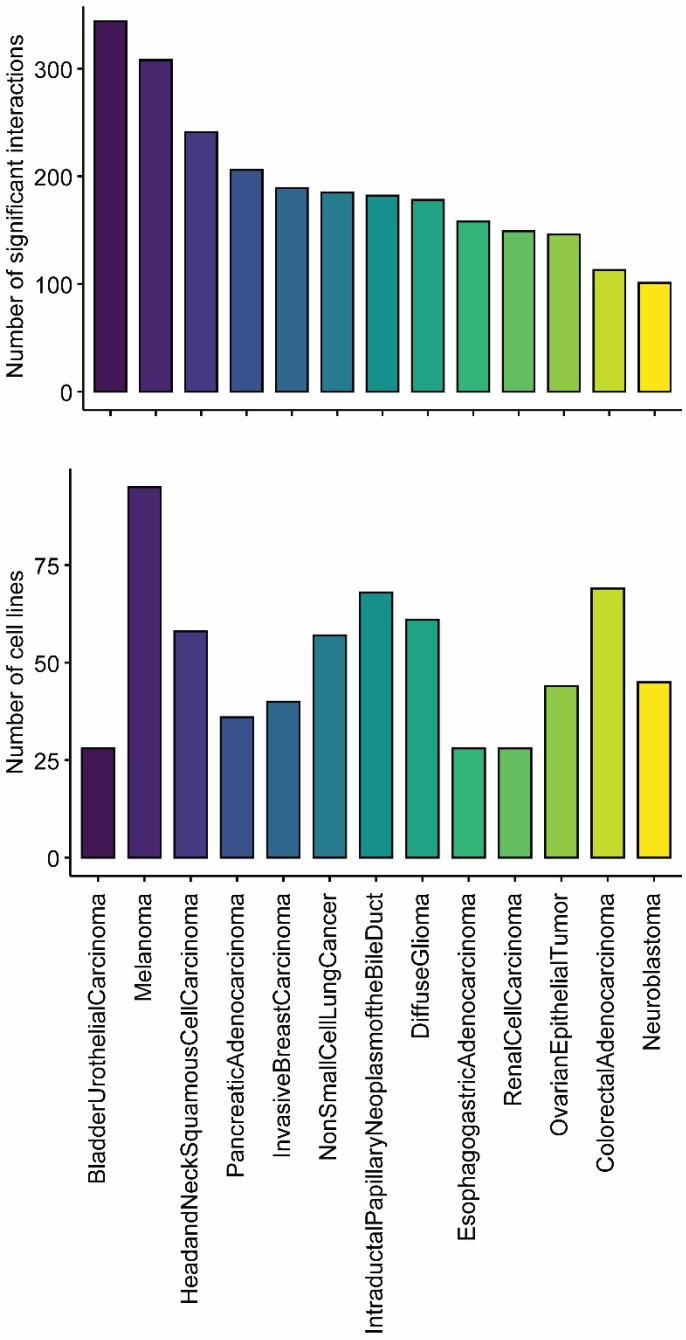

Supplementary Figure 6. Overview of SL interactions identified across cancer types following filtering criteria. **Top)** The number of significant SL interactions per cancer type. **Bottom)** The number of CCLE cell lines available per cancer type. After filtering, a total of 2,500 significant SL interactions were retained across 13 cancer types, including 379 interactions involving a druggable target.

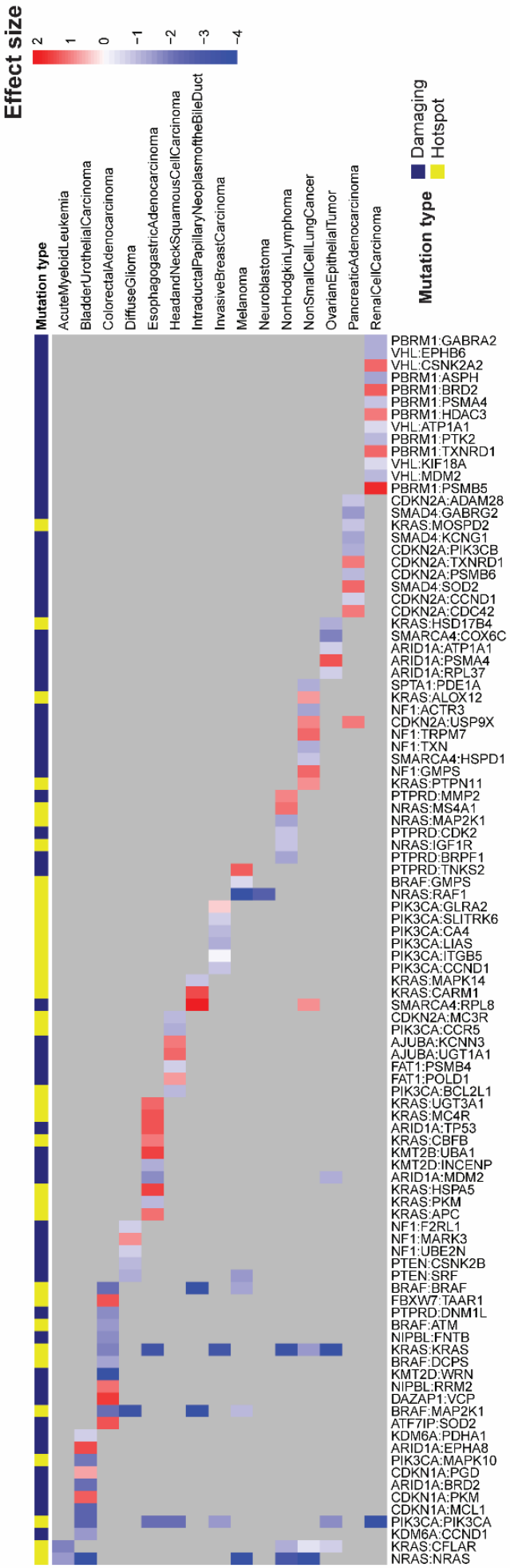

Supplementary Figure 7. Top cancer-specific SL interactions identified across CCLE cell lines. SL interactions between cancer driver genes were computed separately within each cancer type using Boruta RF classifiers, considering only cancer types with ≥25 cell lines having available CRISPR dependency data. For each cancer type, the top seven interactions per feature importance measure were selected, and unique interactions across cancer types were visualized. The heatmap displays the Cohen's d effect size reflecting differences in CRISPR dependency scores between mutated and wild-type cell lines (source driver gene indicated first, target gene second; SOURCE:TARGET). The source mutation type is annotated (left column), distinguishing between damaging mutations (blue) and hotspot mutations (yellow). TP53-driven interactions were excluded to highlight diverse interactions. Complete interaction data are provided in **Supplementary Table 2**

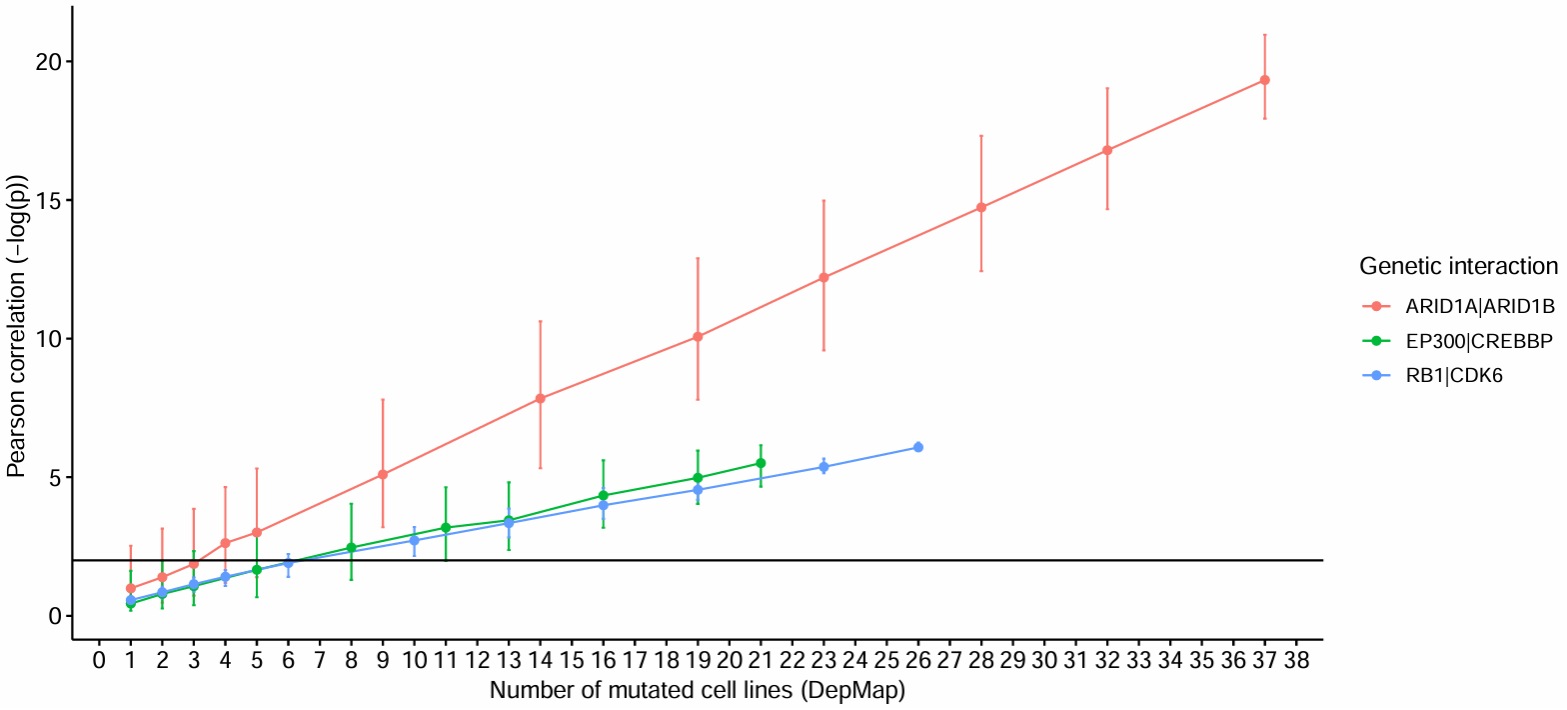

Supplementary Figure 8. Relationship between the statistical significance of SL genetic interactions and the number of mutated cell lines (DepMap). Pearson correlation significance (-log(*P*)) is plotted against the number of cell lines harboring mutations in three known SL gene pairs: *ARID1A*|*ARID1B*, *EP300*|*CREBBP*, and *RB1*|*CDK6*. Error bars represent the standard deviation derived from repeated subsampling. Known SL interactions became consistently significant when source mutations were observed in ≥4 cell lines, justifying this threshold for downstream analysis.